

N92-14350

**EVALUATION OF ROTORDYNAMIC COEFFICIENTS OF LOOK-THROUGH LABYRINTHS  
BY MEANS OF A THREE VOLUME BULK FLOW MODEL**

R. Nordmann and P. Weiser  
Department of Mechanical Engineering  
University of Kaiserslautern  
Kaiserslautern, Federal Republic of Germany

To describe the compressible, turbulent flow in a labyrinth seal, a three volume bulk flow model is presented. The conservation equations for mass, momentum and energy are established in every control volume. A perturbation analysis is performed, yielding zeroth order equations for centric rotor position and first order equations describing the flow field for small rotor motions around the seal center. The equations are integrated numerically. From perturbation pressure, the forces on the shaft and the dynamic coefficients are calculated.

**NOMENCLATURE**

$F_1, F_2$	Forces on the shaft in x,y direction
$u_1, u_2$	shaft displacements
$K, k$	direct and cross-coupled stiffness
$D, d$	direct and cross-coupled damping
$p$	pressure
$u, v, w$	axial, radial and tangential velocity
$T$	temperature
$\rho$	density
$z, r, \varphi$	axial, radial and tangential coordinate
$t$	time
$L$	length of labyrinth chamber
$B$	depth of labyrinth chamber
$R$	shaft radius

$C_r$	nominal clearance
$S$	seal fin thickness
$L_t$	total seal length
$e$	eccentricity ratio, perturbation parameter
$r_o$	radius of circular shaft orbit
$h$	seal clearance
$\omega$	rotational frequency of the shaft
$\Omega$	precession frequency of the shaft
$p_a$	pressure before labyrinth
$p_b$	pressure behind labyrinth
$w_o$	swirl
$R_g$	perfect gas constant
$\kappa$	specific heat ratio
$\tau$	shear stress
$\lambda$	friction factor
$Re$	Reynolds number
$D_H$	hydraulic diameter
$M$	Mach number
$k_{rel}$	relative surface roughness
$\zeta_e$	entrance loss factor
$\zeta_I$	loss factor at seal fin entrance
$\mu$	laminar viscosity
$i$	imaginary unit

## SUBSCRIPTS

0	zeroth order
1	first order
s	stator
r	rotor
z	axial
$\varphi$	circumferential
f	fluid-
cu	chamber, upper wall
cs	chamber, side wall
S	Sine
C	Cosine
e	seal entrance
rel	relative
I,II,III	Indices for the different control volumes

## INTRODUCTION

Labyrinth seals, commonly used in turbomachinery to reduce the leakage loss, can have a strong influence on the dynamic behavior of a turbine or a compressor, especially for high performance machines. In some cases, the fluid forces generated in labyrinths caused severe rotor instabilities. Therefore, the design engineer needs information concerning the possible influences that a labyrinth can have on the dynamics of a rotating system.

For mathematical modeling, the seal forces can be described in terms of stiffness and damping parameters, the so-called rotordynamic seal coefficients (see Eq.1).

$$\begin{bmatrix} K & k \\ -k & K \end{bmatrix} \begin{bmatrix} u_1 \\ u_2 \end{bmatrix} + \begin{bmatrix} D & d \\ -d & D \end{bmatrix} \begin{bmatrix} \dot{u}_1 \\ \dot{u}_2 \end{bmatrix} = - \begin{bmatrix} F_1 \\ F_2 \end{bmatrix} \quad (1)$$

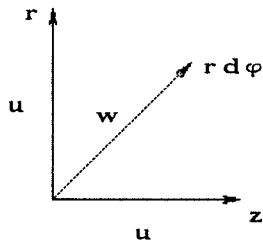
These coefficients are input parameters for rotordynamic investigations and have to be determined by fluid mechanics methods. In contrast to WEISER and NORDMANN (1987,1988,1989), where we used Finite-Differencing methods (FDM) to solve the conservation equations in conjunction with a turbulence model, Florjancic developed a more conventional three volume bulk flow method which takes advantage from FDM calculations and reduces the computational effort dramatically. In 1987, KLAUK has already developed a three volume model for the compressible flow in labyrinths, which is extended in WEISER (1989). In this approach, the energy equation and the equation of state for a perfect gas is used in addition to the previously existing model.

## MATHEMATICAL MODELING

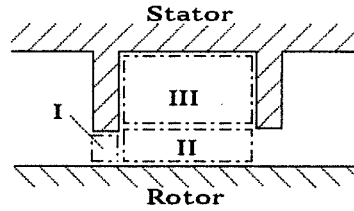
Many attempts have been made for the calculation of labyrinth coefficients, e.g. see the publications of KOSTYUK(1975), CHILDS(1984) or WYSSMANN(1984). Flow visualization experiments show, that for look-through labyrinths, the flow field can be divided in two characteristic regions: a vortex flow in the seal chamber and a jet flow region beneath the seal strip and the groove.

Therefore, the calculation domain is divided into three control volumes (CV), see Fig.1: one in the seal chamber accounting for the vortex flow and two volumes representing the jet flow beneath chamber and seal fin. Fig.1 also gives an impression of the bulk velocities in the different volumes.

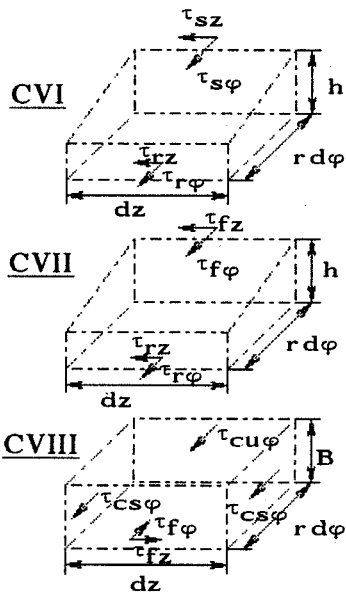
Coordinate System



3-Volume-Model



Control Volumes



0th Order Bulk Velocities

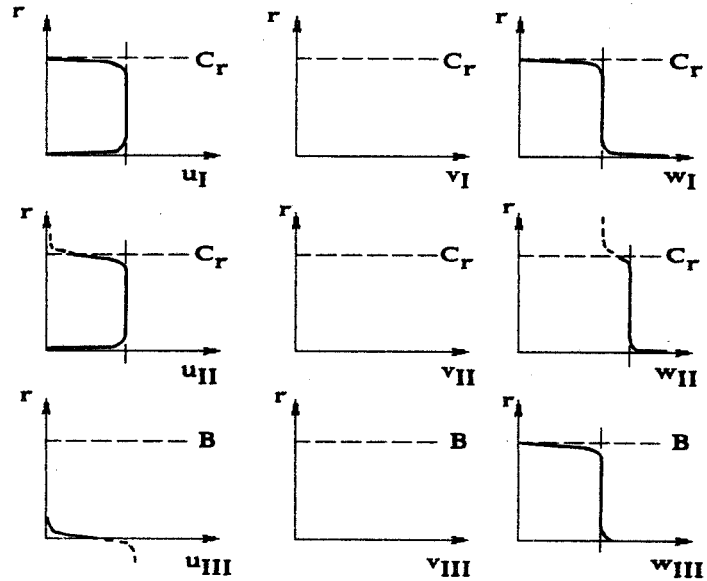


Fig. 1: 3-volume bulk flow model

For mathematical description, we use the momentum, continuity and energy equation in every control volume. Paying attention to the following assumptions:

- compressible medium ( $\rho \neq \text{const.}$ )
- constant laminar viscosity  $\mu$
- modelling of turbulence by wall shear stresses
- no shear stresses within the fluid (exception: jet friction shear stress in the contact region of CV II and CV III)
- no radial shear stresses
- first order radial velocities only in CV II and III

we obtain the following set of equations to describe the turbulent, compressible seal flow (equations shown here for teeth-on-stator seal):

CV I:

$$\begin{aligned}
 -\frac{\partial p}{\partial z} h - \tau_{sz} - \tau_{rz} &= \rho h \left\{ \frac{\partial u}{\partial t} + u \frac{\partial u}{\partial z} + \frac{w}{r} \frac{\partial u}{\partial \varphi} \right\} \\
 -\frac{1}{r} \frac{\partial p}{\partial \varphi} h - \tau_{s\varphi} - \tau_{r\varphi} &= \rho h \left\{ \frac{\partial w}{\partial t} + u \frac{\partial w}{\partial z} + \frac{w}{r} \frac{\partial w}{\partial \varphi} \right\} \\
 0 &= \frac{\partial}{\partial t} \left\{ \frac{p}{x-1} h + \rho h \left( \frac{u^2}{2} + \frac{v^2}{2} + \frac{w^2}{2} \right) \right\} + \\
 &\quad \frac{\partial}{\partial z} \left\{ \rho u h \left( \frac{x}{x-1} \frac{p}{\rho} + \frac{u^2}{2} + \frac{v^2}{2} + \frac{w^2}{2} \right) \right\} + \\
 &\quad \frac{1}{r} \frac{\partial}{\partial \varphi} \left\{ \rho w h \left( \frac{x}{x-1} \frac{p}{\rho} + \frac{u^2}{2} + \frac{v^2}{2} + \frac{w^2}{2} \right) \right\} + \\
 &\quad \tau_{r\varphi} (w - R\omega)
 \end{aligned} \tag{2}$$

$$\begin{aligned}
 0 &= \frac{\partial}{\partial t} (\rho h) + \frac{\partial}{\partial z} (\rho u h) + \\
 &\quad \frac{1}{r} \frac{\partial}{\partial \varphi} (\rho w h)
 \end{aligned}$$

CV II:

$$\begin{aligned}
 -\frac{\partial p}{\partial z} h - \tau_{fz} - \tau_{rz} &= \rho h \left\{ \frac{\partial u}{\partial t} + u \frac{\partial u}{\partial z} + v \frac{\partial u}{\partial r} + \frac{w}{r} \frac{\partial u}{\partial \varphi} \right\} \\
 -\frac{1}{r} \frac{\partial p}{\partial \varphi} h - \tau_{f\varphi} - \tau_{r\varphi} &= \rho h \left\{ \frac{\partial w}{\partial t} + u \frac{\partial w}{\partial z} + v \frac{\partial w}{\partial r} + \frac{w}{r} \frac{\partial w}{\partial \varphi} \right\} \\
 -\frac{\partial p}{\partial r} h &= \rho h \left\{ \frac{\partial v}{\partial t} + u \frac{\partial v}{\partial z} + v \frac{\partial v}{\partial r} + \frac{w}{r} \frac{\partial v}{\partial \varphi} \right\} \\
 0 &= \frac{\partial}{\partial t} \left\{ \frac{p}{x-1} h + \rho h \left( \frac{u^2}{2} + \frac{v^2}{2} + \frac{w^2}{2} \right) \right\} + \\
 &\quad \frac{\partial}{\partial z} \left\{ \rho u h \left( \frac{x}{x-1} \frac{p}{\rho} + \frac{u^2}{2} + \frac{v^2}{2} + \frac{w^2}{2} \right) \right\} + \\
 &\quad \frac{1}{r} \frac{\partial}{\partial \varphi} \left\{ \rho w h \left( \frac{x}{x-1} \frac{p}{\rho} + \frac{u^2}{2} + \frac{v^2}{2} + \frac{w^2}{2} \right) \right\} + \\
 &\quad \frac{\partial}{\partial r} \left\{ \rho v h \left( \frac{x}{x-1} \frac{p}{\rho} + \frac{u^2}{2} + \frac{v^2}{2} + \frac{w^2}{2} \right) \right\} + \\
 &\quad \tau_{r\varphi} (w - R\omega)
 \end{aligned} \tag{3}$$

$$0 = \frac{\partial}{\partial t}(\rho h) + \frac{\partial}{\partial z}(\rho u h) + \frac{1}{r} \frac{\partial}{\partial \varphi}(\rho w h) + \frac{\partial}{\partial r}(r \rho v h)$$

CV III:

$$-\frac{\partial p}{\partial z} B + \tau_{fz} - \tau_{cu z} = 0$$

$$-\frac{1}{r} \frac{\partial p}{\partial \varphi} - \frac{2B}{L} \tau_{cs\varphi} - \tau_{cu\varphi} + \tau_{f\varphi} = \rho B \left\{ \frac{\partial w}{\partial t} + v \frac{\partial w}{\partial r} + \frac{w}{r} \frac{\partial w}{\partial \varphi} \right\} \quad (4)$$

$$-\frac{\partial p}{\partial r} B = \rho B \left\{ \frac{\partial v}{\partial t} + v \frac{\partial v}{\partial r} + \frac{w}{r} \frac{\partial v}{\partial \varphi} \right\}$$

$$0 = \frac{\partial}{\partial t}(\rho B) + \frac{1}{r} \frac{\partial}{\partial \varphi}(\rho w B) + \frac{\partial}{\partial r}(r \rho v B)$$

As already mentioned, the modeling of flow turbulence is performed using semi-empirical wall shear stress formulations which is the usual way in bulk flow analysis, see for example CHILDS(1984), SCHARRER(1987). The fluid shear stress in the contact region of CV II and CV III is described in the same manner as WYSSMANN(1984) suggested. All shear stress components can be written in a generalized form:

$$\tau_{ij} = \frac{1}{2} \rho \lambda_i V_j V_{rel}$$

with

$$\lambda_i = n \left\{ 1 + \left[ C_1 k_{rel} + \frac{C_2}{Re} \right]^m \right\} \quad (5)$$

and

$$Re = \frac{D_H V_{rel}}{\mu/\rho}$$

$V_{rel}$  is the relative velocity,  $V_j$  the component of the resulting velocity vector which is in the same direction as the shear stress component to be calculated. Index  $i$  indicates the appropriate shear stress ( $s$ : stator-,  $r$ : rotor etc.) and index  $j$  gives the direction ( $z$ : axial,  $\varphi$ : tangential). With these definitions, we obtain the following relations:

CV I:

$$\begin{array}{ll} \text{Rotor:} & V_{\text{rel}} = \left( (w_I - R\omega)^2 + u_I^2 \right)^{0.5} \\ & V_{\varphi} = w_I - R\omega \\ & V_z = u_I \\ \text{Stator:} & V_{\text{rel}} = \left( w_I^2 + u_I^2 \right)^{0.5} \\ & V_{\varphi} = w_I \\ & V_z = u_I \end{array}$$

CV II:

$$\begin{array}{ll} \text{Rotor:} & V_{\text{rel}} = \left( (w_{II} - R\omega)^2 + u_{II}^2 \right)^{0.5} \\ & V_{\varphi} = w_{II} - R\omega \\ & V_z = u_{II} \\ \text{Stator:} & V_{\text{rel}} = \left( w_{II}^2 + u_{II}^2 \right)^{0.5} \\ & V_{\varphi} = w_{II} \\ & V_z = u_{II} \end{array}$$

$$\begin{array}{l} \text{Jet:} \\ V_{\text{rel}} = \left( (w_{II} - w_{III})^2 + (u_{II} - u'_{III})^2 \right)^{0.5} \text{ with } u'_{III} = u_{II} (1 - \beta_v) \\ V_{\varphi} = w_{II} - w_{III} \\ V_z = u_{II} - u'_{III} \end{array}$$

(6)

CV III:

$$\begin{array}{l} \text{Jet:} \\ V_{\text{rel}} = \left( (w_{II} - w_{III})^2 + (u_{II} - u'_{III})^2 \right)^{0.5} \\ V_{\varphi} = w_{II} - w_{III} \\ V_z = u_{II} - u'_{III} \end{array}$$

Chamber side wall:

$$\begin{array}{l} V_{\text{rel}} = \left( w_{III}^2 + u''_{III}{}^2 \right)^{0.5} \text{ with } u''_{III} = u'_{II} \frac{B}{L} \\ V_{\varphi} = w_{III} \end{array}$$

Upper wall in the seal groove:

$$\begin{array}{l} V_{\text{rel}} = \left( w_{III}^2 + u'_{III}{}^2 \right)^{0.5} \\ V_{\varphi} = w_{III} \\ V_z = u'_{III} \end{array}$$

The parameters introduced in the shear stress formulations according to MOODY (1944) are

$$n=0.001375$$

$$m=0.33333$$

$$C_1=10^4$$

$$C_2=10^6$$

For the fluid shear stress,  $m$ ,  $C_1$  and  $C_2$  are zero;  $n$  is set to 3.762 (according to WYSSMANN). To account for the real flow situation in the labyrinth,  $n$  is multiplied with the factor  $\beta$ , which depends on geometry and performance data.

### BOUNDARY CONDITIONS

For the solution of the differential equations, boundary conditions have to be specified. To calculate the pressure, density and axial velocity at the seal entrance, we use the same relations as NELSON(1985), calculating the entrance values depending on the Mach number:

$$p_e = p_a \left[ 1 + \frac{(\chi-1)(\zeta_e+1)}{2} M_e^2 \right]^{\frac{\chi}{1-\chi}}$$

$$\rho_e = \rho_a \left[ 1 + \frac{(\chi-1)}{2} M_e^2 \right] \left[ 1 + \frac{(\chi-1)(\zeta_e+1)}{2} M_e^2 \right]^{\frac{\chi}{1-\chi}} \quad (7)$$

$$T_e = \frac{p_e}{R_g \rho_e} \quad M_e = \frac{u_e}{\sqrt{\chi R_g T_e}}$$

$$\zeta_e = \sqrt{\frac{5.3}{\lg(\text{Re})}} - 1$$

At the entrance of every seal fin, there occurs a pressure drop due to the acceleration of the fluid. Therefore, the equations 7 are used in a modified form with a constant loss factor  $\zeta_I$ :



$$\begin{aligned}
p_I &= p_{II} \left[ 1 + \frac{(\alpha-1)(\zeta_I+1)}{2} M_{II}^2 \right]^{\frac{\alpha}{1-\alpha}} \\
\rho_I &= \rho_{II} \left[ 1 + \frac{(\alpha-1)}{2} M_{II}^2 \right] \left[ 1 + \frac{(\alpha-1)(\zeta_I+1)}{2} M_{II}^2 \right]^{\frac{\alpha}{1-\alpha}} \\
T_{II} &= \frac{p_{II}}{R_g \rho_{II}} \quad M_{II} = \frac{u_{II}}{\sqrt{\alpha R_g T_{II}}}
\end{aligned} \tag{8}$$

The model parameters  $\beta$ ,  $\beta_v$  and  $\zeta_I$  are determined with the help of the Finite-Difference programs of NORDMANN and WEISER(1987,1988,1989).

### PERTURBATION ANALYSIS

In order to determine the seal forces, we assume that the rotor performs only small motions around the seal center. Then we can describe the dependent variables with a perturbations series, truncated after the linear term:

$$\begin{aligned}
u &= u_0 + e u_1 & p &= p_0 + e p_1 & h &= C_r + e h_1 \\
v &= v_0 + e v_1 & T &= T_0 + e T_1 \\
w &= w_0 + e w_1 & \rho &= \rho_0 + e \rho_1
\end{aligned} \tag{9}$$

As perturbation parameter, we choose the relative eccentricity  $e$ , which is the ratio of the shaft eccentricity and the nominal clearance:

$$e = \frac{r_0}{C_r} \tag{10}$$

Inserting these expressions into the governing equations, separating terms without  $e$  and with  $e^1$  yields two sets of equations: the zeroth order relations describe the flow field for a centric rotor position and the first order terms stand for the flow situation at small eccentric shaft motion.

## ELIMINATION OF TEMPORAL AND CIRCUMFERENTIAL DERIVATIVES

While the zeroth order equations depend only on the axial coordinate  $z$ , the first order set contains also derivatives with respect to time  $t$ , tangential and radial coordinates. Assuming that the shaft moves on a small circular orbit (see Fig. 2), the seal clearance can be written as

$$h = h_0 + e h_1 = C_r - X(t) \cos\varphi - Y(t) \sin\varphi \quad (11)$$

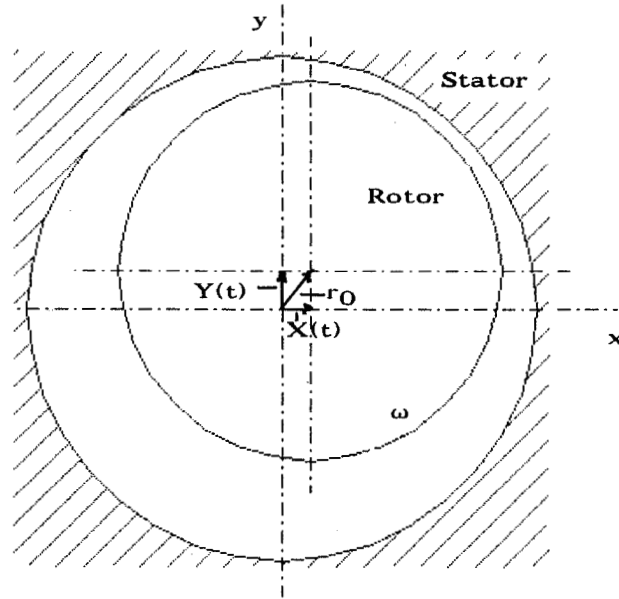


Fig. 2: Circular shaft orbit

For the dependent variables, we prescribe a corresponding solution:

$$\begin{aligned} u_1 &= u_{1c} \cos\varphi + u_{1s} \sin\varphi & p_1 &= p_{1c} \cos\varphi + p_{1s} \sin\varphi \\ v_1 &= v_{1c} \cos\varphi + v_{1s} \sin\varphi & T_1 &= T_{1c} \cos\varphi + T_{1s} \sin\varphi \\ w_1 &= w_{1c} \cos\varphi + w_{1s} \sin\varphi & \rho_1 &= \rho_{1c} \cos\varphi + \rho_{1s} \sin\varphi \end{aligned} \quad (12)$$

Now, the circumferential derivatives can be calculated analytically. Separating the equations with respect to sine and cosine terms and introducing complex variables:

$$\begin{aligned}
\bar{u}_1 &= u_{1c} + i u_{1s} & \bar{p}_1 &= p_{1c} + i p_{1s} \\
\bar{v}_1 &= v_{1c} + i v_{1s} & \bar{T}_1 &= T_{1c} + i T_{1s} \\
\bar{w}_1 &= w_{1c} + i w_{1s} & \bar{\rho}_1 &= \rho_{1c} + i \rho_{1s}
\end{aligned} \tag{13}$$

we obtain a now complex system of first order equations.

As already mentioned, we assume a circular shaft orbit, which gives for the time dependence of the clearance

$$\bar{h}_1 = r_0 e^{i\Omega t} \tag{14}$$

Again, similar expressions for the variables are established:

$$\begin{aligned}
\bar{u}_1 &= \hat{u}_1 e^{i\Omega t} & \bar{w}_1 &= \hat{w}_1 e^{i\Omega t} & \bar{T}_1 &= \hat{T}_1 e^{i\Omega t} \\
\bar{v}_1 &= \hat{v}_1 e^{i\Omega t} & \bar{p}_1 &= \hat{p}_1 e^{i\Omega t} & \bar{\rho}_1 &= \hat{\rho}_1 e^{i\Omega t}
\end{aligned} \tag{15}$$

Thereby, the derivatives with respect to time can be expressed analytically. Finally, the radial derivatives in CV II and III are modeled with

$$\begin{aligned}
\frac{\partial \hat{v}_{II}}{\partial r} &= \frac{(\rho_{III0} \hat{v}_{III1} - \rho_{II0} \hat{v}_{II1})}{\rho_{II0} C_r} \\
\frac{\partial \hat{v}_{III}}{\partial r} &= - \frac{(\rho_{III0} \hat{v}_{III1} - \rho_{II0} \hat{v}_{II1})}{\rho_{III0} B}
\end{aligned} \tag{16}$$

After having performed these steps, the first order equations do only depend on  $z$ . The solution starts with a numerical integration of zeroth order equations

with respect to the boundary conditions. The first order solution using the perturbed boundary conditions yields the pressure distribution in the seal for small rotor motions. The forces are obtained by a pressure integration:

$$F_1 = - \int_0^{L_t} \int_0^{2\pi} p \cos \varphi r d\varphi dz = - r_0 \frac{\pi r}{C_r} \int_0^{L_t} p_{1c} dz$$

$$F_2 = - \int_0^{L_t} \int_0^{2\pi} p \sin \varphi r d\varphi dz = - r_0 \frac{\pi r}{C_r} \int_0^{L_t} p_{1s} dz$$
(17)

Because we have to determine 4 parameters (K, k, D, d), the calculation of first order equations has to be done twice for two different rotor precession frequencies ( $\Omega=0$  and  $\Omega=\omega$ ). Then the rotordynamic coefficients can be calculated:

$$K + \Omega d = \frac{\pi r}{C_r} \int_0^{L_t} p_{1c} dz$$

$$-k + \Omega D = \frac{\pi r}{C_r} \int_0^{L_t} p_{1s} dz$$
(18)

## COMPARISON TO EXPERIMENTS AND OTHER BULK-FLOW-THEORIES

### 1. Example

BENCKERT(1980) investigated experimentally a three chamber look-through labyrinth. Due to the design of his test rig, he could only measure stiffnesses. The data of the labyrinth are

R : 150 mm  
 L : 7.75 mm  
 B : 5.5 mm  
 S : 0.25 mm  
 C<sub>r</sub>: 0.5 mm  
 p<sub>a</sub>: 1.425 bar  
 p<sub>b</sub>: 0.953 bar

T<sub>a</sub>: 300 K  
 working fluid: air  
 number of chambers : 3  
 No shaft rotation !

Fig.3 and 4 show the comparison to the experimental data for different preswirl conditions. While the 3-volume approach predicts a positive direct stiffness according to the measurements, the theory of CHILDS(1984) gives the opposite sign for K. The agreement between experiment and 3-volume model is good, especially showing that the model presented is capable to ensure sufficient accuracy in the calculation of dynamic seal parameters even for short labyrinth seals where the approaches of CHILDS or WYSSMANN have some problems.

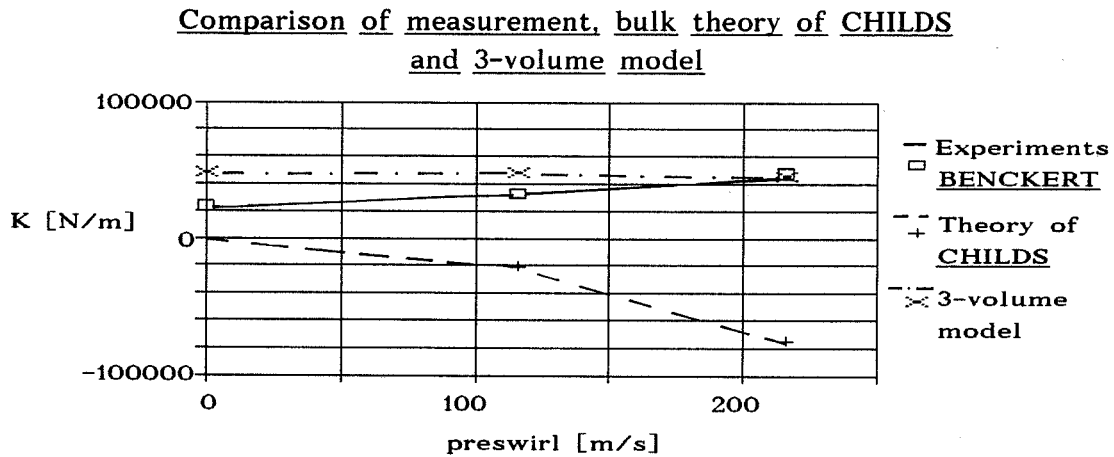


Fig. 3: Direct stiffness K

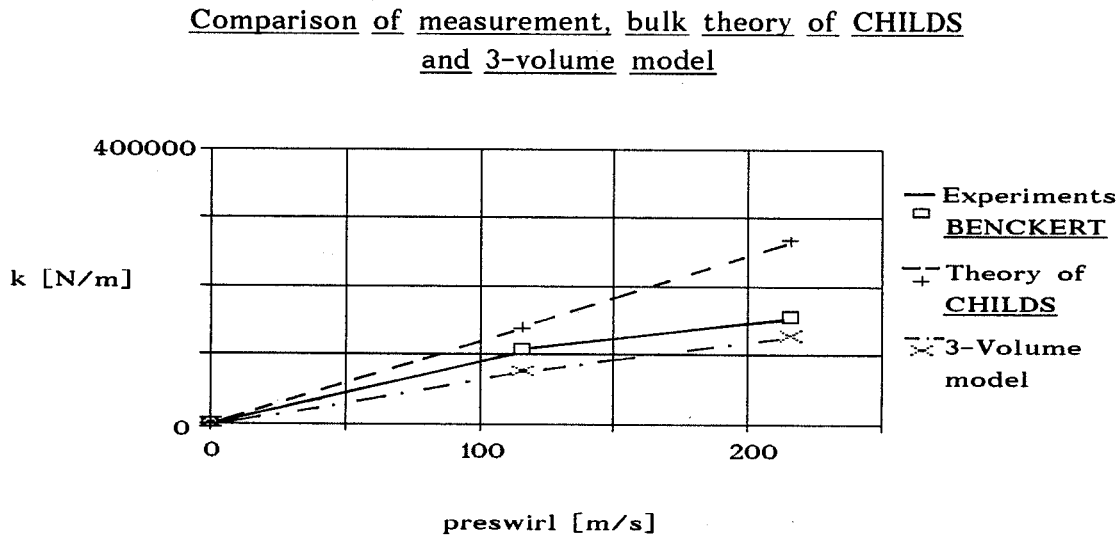


Fig. 4: Cross-coupled stiffness k

## 2. Example

In a paper published 1986, WYSSMANN shows a comparison of measured data for a 15-chamber look-through labyrinth. The experiments were carried out by CHILDS(1984). WYSSMANN compares the measurements to his 2-volume approach. For a 16-strip seal with fins on stator, the results of the experiments, of WYSSMANN and the 3-volume model are shown in Fig. 5 - 7.

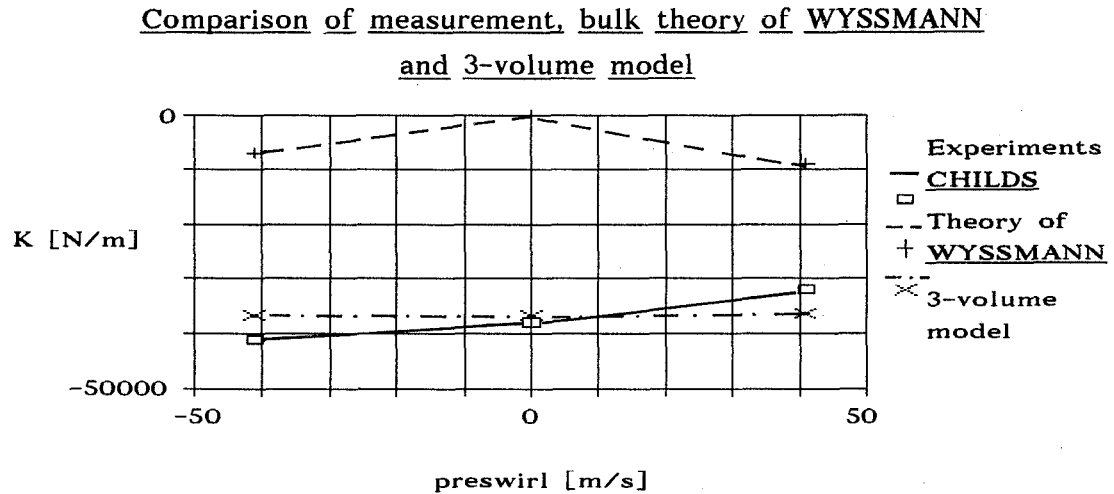


Fig. 5: Direct stiffness

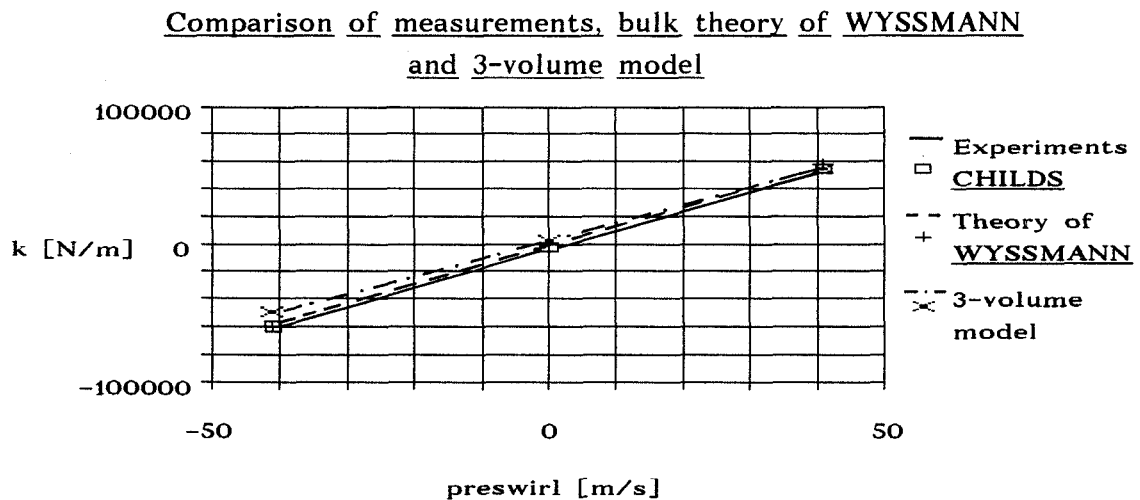


Fig. 6: Cross-coupled stiffness

Comparison of measurement, bulk theory of WYSSMANN  
and 3-volume model

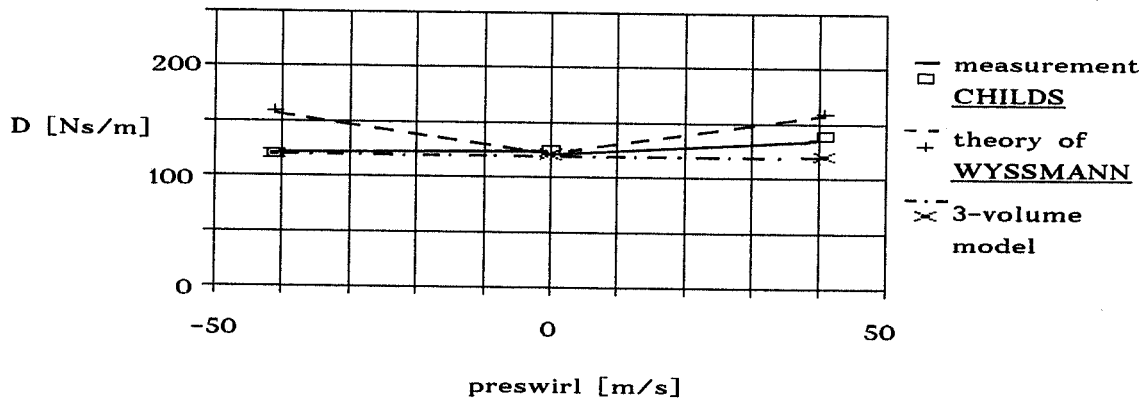


Fig. 7: Direct damping

In contrast to the 2-volume theory, the model presented here predicts the direct stiffness more accurate.

## CONCLUSION

A new bulk flow model has been presented for the calculation of the rotor-dynamic seal parameters. The theory uses a three volume approach, and conservation equations for mass, momentum and energy are set up for every control volume. A perturbation analysis yields zeroth and first order equations. The integration of first order pressure perturbation results in the desired dynamic coefficients.

The comparison to experiments shows good agreement; compared to other bulk flow models, the present theory allows a much better calculation of the direct stiffness. This is mostly due to the determination of the model parameters with the help of the FDM programs, as a comparison to an earlier 3-volume model of KLAUK, which was developed in 1987 and did not have the benefit of using FDM results, shows.

## REFERENCES

BENCKERT, H.:

"Strömungsbedingte Federkennwerte in Labyrinthdichtungen"  
Dissertation TU Stuttgart, 1980

CHILDS, D. W., SCHARRER, J. K.:

"An Iwatsubo Solution for Labyrinth Seals Comparison of  
Experimental Results"  
NASA 2338, May 1984

CHILDS, D.W.; SCHARRER, J.K.:

"Experimental Rotordynamic Coefficients Results for Teeth-on-Rotor-  
and Teeth-on-Stator Labyrinth Gas Seals"  
NASA CP 2443, 1986, p.259-276

FLORJANCIC, S.:

"Annular Seals of High Energy Centrifugal Pumps"  
Dissertation, Swiss Federal Institute of Zurich, 1990

KLAUK, E.:

"Berechnung der rotordynamischen Koeffizienten von mit kompressiblen  
Medien durchströmten Labyrinthdichtungen unter Anwendung von  
Mehr-Volumen-Modellen"  
Diplomarbeit, University of Kaiserslautern, 1987; AG Machine Dynamics

KOSTYUK, A. G.:

"Circulation Forces over the Shrouding and their Influence on the  
Threshold Capacity of Large Turbine Units"  
Teploenergetika, 1975, Vol.22, No.3, p. 41-46

MOODY, L. F.:

"Friction Factors for Pipe Flow"  
Trans. ASME 66 (November 1944), p. 671-684

NELSON, C. C.:

"Rotordynamic Coefficients for Compressible Flow in Tapered Annular  
Seals"  
Journal of Tribology, Vol 107, July 1985



NORDMANN, R., DIETZEN, F. J., WEISER, H. P.:

"Calculation of Rotordynamic Coefficients and Leakage for Annular Gas Seals by Means of Finite-Difference Techniques"

11th Biennial Conference on Mechanical Vibration and Noise,  
Boston, 27-30 Sept. 1987

NORDMANN, R., WEISER, H.P.:

"Rotordynamic Coefficients for Labyrinth Seals Calculated by Means of a Finite-Difference Technique"

NASA, CP 3026, 1988

SCHARRER, J. K.:

"Theory versus Experiment for the Rotordynamic Coefficients of Labyrinth Gas Seals: Part I - A Two Control Volume Model"

The 11th Biennial Conference on Mechanical Vibrations and Noise,  
Boston, 27-30 Sept. 1987

WEISER, H. P., NORDMANN, R.:

"Calculation of Rotordynamic Labyrinth Seal Coefficients by Means of a Threedimensional Finite-Difference Method"

Accepted for presentation for: 12th Biennial Conference on Mechanical Vibration and Noise, Montreal, Sept. 1989

WEISER, H. P.:

"Ein Beitrag zur Berechnung der dynamischen Koeffizienten von Labyrinthdichtungssystemen bei turbulenter Durchströmung mit kompressiblen Medien"

Ph. D. Thesis, University of Kaiserslautern 1989

WYSSMANN, H. R., PHAM, T. C., JENNY, R. J.:

"Prediction of Stiffness and Damping Coefficients for Centrifugal Compressor Labyrinth Seals"

ASME Journal of Engineering for Gas Turbines and Power,  
Oct. 1984, B. 106, p. 920-926

WYSSMANN, H.R.:

"Theory and Measurement of Labyrinth Gas Seal Coefficients for Rotor Stability of Turbocompressors"

NASA CP 2443, 1986, p.237-258